J. Appl. Math. & Informatics Vol. **40***(2022), No. 1 - 2, pp. 99 - 115*
https://doi.org/10.14317/jami.2022.099

INFLUENCE OF CONSTANT HEAT SOURCE/SINK ON NON-DARCIAN-BENARD DOUBLE DIFFUSIVE MARANGONI CONVECTION IN A COMPOSITE LAYER SYSTEM

N. MANJUNATHA*, R. SUMITHRA AND R.K. VANISHREE

Abstract. The problem of Benard double diffusive Marangoni convection is investigated in a horizontally infinite composite layer system consisting of a two component fluid layer above a porous layer saturated with the same fluid, using Darcy-Brinkman model with constant heat sources/sink in both the layers. The lower boundary of the porous region is rigid and upper boundary of the fluid region is free with Marangoni effects. The system of ordinary differential equations obtained after normal mode analysis is solved in closed form for the eigenvalue, thermal Marangoni number for two types of thermal boundary combinations, Type (I) Adiabatic-Adiabatic and Type (II) Adiabatic -Isothermal. The corresponding two thermal Marangoni numbers are obtained and the essence of the different parameters on non-Darcy-Benard double diffusive Marangoni convection are investigated in detail.

AMS Mathematics Subject Classification : 80-XX, 80Axx, 80A20.
Key words and phrases : Heat source/sink, double diffusive convection, composite layer, Adiabatic-Adiabatic, Adiabatic-Isothermal, depth ratio.

1. Introduction

Double diffusive convection is a convection, which has a combination of two density gradients diffusing at diverse rates. The presence of double diffusive convection in natural processes is evident like in sea water, the mantle flow in the Earth's crust and has a bundle of engineering applications. For example, contaminant transport in saturated soils, food processing, spread of toxins and furthermore appears in the modeling of solar ponds and crystal growth industries. Marangoni convection resulting from the local variation of surface tension due to a non-uniform temperature distribution is an interesting fluid mechanical problem. The problems of double diffusive convection in single fluid /porous

Received March 12, 2021. Revised July 5, 2021. Accepted July 19, 2021. *Corresponding author.
© 2022 KSCAM.

/two layers / heat source/sink are investigated by some authors. Shivakumara and Sumithra [17] have studied the linear and non-linear stability of double diffusive convection in a sparsely packed porous layer using the Brinkmann model and simple and Hopf bifurcations are obtained in the case of linear theory conditions. Khanafer & Vafai [7] studied mixed-convection of temperature and concentration transport in a lid-driven square enclosure filled in a layer of non-Darcian fluid saturated porous medium numerically by choosing insulated two vertical walls of the enclosure, keeping the horizontal walls at constant but different heat and salinity with the upper layer moving at a constant speed. Khalili and Shivakumara [6] investigated the effect of vertical through flow on thermal convective instabilities in a porous layer using Brinkman extended Darcy model including Lapwood and Forchheimer inertia terms with fluid viscosity being different from effective viscosity by considering different boundary conditions which are either conducting or insulating to temperature perturbations. Krishna B. Chavaraddi [8] have considered the linear stability analysis of Marangoni convection in a composite system comprised of an incompressible fluid-saturated porous layer underlying a layer of the same fluid with the upper fluid surface, free to the atmosphere and deformable, subjected to temperature-dependent surface tension. Baytas *et al.*[2] have investigated the double diffusive natural convection between a saturated porous layer and an overlying fluid layer in an enclosure using the non-Darcy flow model. Sankar *et al.* [15] studied the natural convection flows in a vertical annulus filled with a fluid-saturated porous medium has been investigated when the inner wall is subject to discrete heating. Numerical study of double-diffusive natural convective heat and mass transfer in an inclined rectangular cavity filled with a porous medium by Khaled. Al-Farhany and Turan [4].Sankar *et al.* [16] studied the natural convection in a vertical annulus filled with a fluid-saturated porous medium, and with internal heat generation subject to a discrete heating from the inner wall. Benard convection in a porous medium using the non-Darcy model with localized heating is studied numerically by Habibis Saleh and Ishak Hashim [3]. Nield and Bejan [12] have investigated the effects of both weak and strong heterogeneity on the onset of double-diffusive convection which is induced by combined effects of internal heating and solutal gradient by considering a composite porous medium consisting of two horizontal layers. Laminar natural convection inside a square composite vertically layered cavity is studied numerically by Muneer A. Ismael and Ali J. Chamkha [11] using under a successive relaxation upwind-scheme finite difference method also, Darcy Brinkman model for the porous layer.

Recently, Akil J. Harfash and Fahad K. Nashmi [1] studied double-diffusive convection when there is a heat sink/source which is linear in the vertical coordinate in the opposite direction to gravity by considering a horizontal fluid layer. The thresholds for linear instability are found and compared to those derived by a global nonlinear energy stability analysis. Safi and Benissaad [14] discussed the double diffusive natural convection in an anisotropic porous medium saturated with a binary fluid using Darcy Brinkman Forchheimer model with the

Boussinesq approximation employing finite volume method to solve the governing equations. Manjunatha and Sumithra [9] have discussed the double diffusive convection in the presence of three temperature gradients. Khaled Al-Farhany and Turan [5] experimentally investigated the mixed convection in a square enclosure partitioned in two layers. The results showed that the effect of cylinder rotation was around cylinder only. Rashmi Dubey and Murthy [13] studied the onset of double-diffusive convection in a highly permeable porous medium with a horizontal throughflow is investigated by considering the convective thermal boundary conditions. Manjunatha and Sumithra [10] have discussed the single component convection in the presence of heat source and temperature gradients.

In this paper, the problem of Benard double diffusive Marangoni convection is investigated in a horizontally infinite two layer system consisting of a two component fluid layer above a porous layer saturated with the same fluid, for Darcy-Brinkmann model with constant heat sources in both the layers under microgravity condition. The lower boundary of the porous region is rigid and upper boundary of the fluid region is free with Marangoni effects. The system of ordinary differential equations obtained after normal mode analysis is solved in closed form for the eigenvalue, Thermal Marangoni number for two types of thermal boundary combinations, Type (I) Adiabatic-Adiabatic and Type (II) Adiabatic-Isothermal. The corresponding two thermal Marangoni numbers M_{t1} & M_{t2} are obtained and the impact of the porous parameter, solute Marangoni number, modified internal Rayleigh numbers, Viscosity ratio and the diffusivity ratio on non Darcy-Benard double diffusive Marangoni convection, are investigated in detail.

2. Mathematical Formulation

The two layer system under investigation is shown in Figure 1. Consider a horizontal two component, fluid saturated isotropic incompressible sparsely packed porous layer of thickness d_m underlying a two component fluid layer of thickness d with constant heat sources Q_m and Q respectively. The lower surface of the porous layer rigid and the upper surface of the fluid layer is free with surface tension effects depending on temperature and concentration. Both the boundaries are kept at different constant temperatures and salinities. A Cartesian coordinate system is chosen with the origin at the interface between porous and fluid layers and the z-axis, vertically upwards. The basic equations for fluid and porous layer respectively governing such a system are,

$$\nabla.\overrightarrow{V} = 0 \tag{1}$$

$$\rho_0[\frac{\partial \overrightarrow{V}}{\partial t} + (\overrightarrow{V}.\nabla)\overrightarrow{V}] = -\nabla P + \mu\nabla^2\overrightarrow{V} \tag{2}$$

$$\frac{\partial T}{\partial t} + (\overrightarrow{V}.\nabla)T = \kappa\nabla^2 T + Q \tag{3}$$

$$\frac{\partial C}{\partial t} + (\overrightarrow{V}.\nabla)C = \kappa_c\nabla^2 C \tag{4}$$

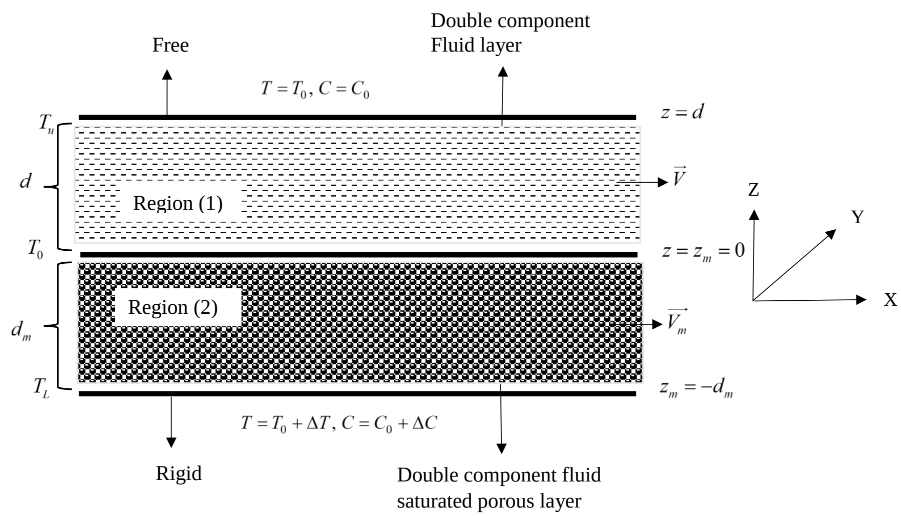

FIGURE 1. Geometry of the problem

$$\nabla_m.\overrightarrow{V_m} = 0 \tag{5}$$

$$\rho_0[\frac{1}{\phi}\frac{\partial \overrightarrow{V_m}}{\partial t} + \frac{1}{\phi^2}(\overrightarrow{V_m}.\nabla_m)\overrightarrow{V_m}] = -\nabla_m P_m - \frac{\mu}{K}\overrightarrow{V_m} + \mu_m \nabla_m^2 \overrightarrow{V_m} \tag{6}$$

$$A\frac{\partial T_m}{\partial t} + (\overrightarrow{V_m}.\nabla_m)T_m = \kappa_m \nabla_m^2 T_m + Q_m \tag{7}$$

$$\phi\frac{\partial C_m}{\partial t} + (\overrightarrow{V_m}.\nabla_m)C_m = \kappa_{cm} \nabla_m^2 C_m \tag{8}$$

Here $\overrightarrow{V}$, ρ_0, μ, μ_m P, T, κ , κ_c, C, K, A, ϕ are namely, the velocity vector, the fluid density, the fluid viscosity, the effective viscosity of the fluid in the porous layer, the pressure, the temperature, the thermal diffusivity of the fluid, the solute diffusivity of the fluid, the concentration, the permeability of the porous medium, the ratio of heat capacities and the porosity respectively and the subscript 'm' refer to the quantities in porous layer.
The basic state is quiescent, have the following solutions
Fluid layer:

$$\overrightarrow{V} = 0, P = P_b(z), T = T_b(z), C = C_b(z) \tag{9}$$

Porous layer:

$$\overrightarrow{V_m} = 0, P_m = P_{mb}(z_m), T_m = T_{mb}(z_m), C_m = C_{mb}(z_m) \tag{10}$$

The temperature distribution in the basic state are obtained by

$$\left.\begin{aligned} T_b(z) = \frac{-Qz(z-d)}{2\kappa} + \frac{(T_u - T_0)z}{d} + T_0 \\ in \quad 0 \le z \le d \end{aligned}\right\} \tag{11}$$

$$\left.\begin{aligned} T_{mb}(z_m) = \frac{-Q_m z_m(z_m + d_m)}{2\kappa_m} + \frac{(T_0 - T_l)z_m}{d_m} + T_0 \\ in \quad -d_m \le z_m \le 0 \end{aligned}\right\} \tag{12}$$

The concentration distributions in the basic state are obtained by

$$\left. C_b(z) = C_0 - \frac{(C_0 - C_u)z}{d} \quad in \quad 0 \le z \le d \right\} \tag{13}$$

$$\left. C_{mb}(z_m) = C_0 - \frac{(C_l - C_0)z_m}{d_m} \quad in \quad -d_m \le z_m \le 0 \right\} \tag{14}$$

where $T_0 = \dfrac{\kappa d_m T_u + \kappa_m d T_l}{\kappa d_m + \kappa_m d} + \dfrac{d d_m(Q_m d_m + Qd)}{2(\kappa d_m + \kappa_m d)}$, $C_0 = \dfrac{\kappa_c d_m C_u + \kappa_{cm} d C_l}{\kappa_c d_m + \kappa_{cm} d}$ are the interface temperature and concentration respectively.

To investigate the stability of the basic state, infinitesimal disturbances are superimposed on fluid and porous layer respectively

$$\left. \overrightarrow{V} = \overrightarrow{V}', P = P_b + P', T = T_b(z) + \theta, C = C_b(z) + S \right\} \tag{15}$$

$$\left. \overrightarrow{V_m} = \overrightarrow{V_m}', P_m = P_{mb} + P'_m, T_m = T_{mb}(z_m) + \theta_m, C_m = C_{mb}(z_m) + S_m \right\} \tag{16}$$

Following the standard linear stability analysis procedure and assuming that the principle of exchange of stability holds (Manjunatha and Sumithra [9, 10]), we arrive at the following stability equations:

in $0 \le z \le 1$

$$(D^2 - a^2)^2 W(z) = 0 \tag{17}$$

$$(D^2 - a^2)\theta(z) + [1 + R_I^*(2z - 1)]W(z) = 0 \tag{18}$$

$$\tau(D^2 - a^2)S(z) + W(z) = 0 \tag{19}$$

in $-1 \le z_m \le 0$

$$[(D_m^2 - a_m^2)\hat{\mu}\beta^2 - 1](D_m^2 - a_m^2)W_m(z_m) = 0 \tag{20}$$

$$(D_m^2 - a_m^2)\theta_m(z_m) + [1 + R_{Im}^*(2z_m + 1)]W_m(z_m) = 0 \tag{21}$$

$$\tau_{pm}(D_m^2 - a_m^2)S_m(z_m) + W_m(z_m) = 0 \tag{22}$$

Here, $R_I^* = \dfrac{R_i}{2(T_0 - T_u)}$, $R_i = \dfrac{Qd^2}{\kappa}$, $\tau = \dfrac{\kappa_c}{\kappa}$ are namely, the modified internal Rayleigh number, the internal Rayleigh number, the diffusivity ratio for fluid layer respectively and $\widehat{\mu} = \dfrac{\mu_m}{\mu}$, $\beta^2 = \frac{K}{d_m^2} = Da$, β, $R_{Im}^* = \dfrac{R_{im}}{2(T_l - T_0)}$, $R_{im} =$

$\frac{Q_m d_m^2}{\kappa_m}$, $\tau_{pm} = \frac{\kappa_{cm}}{\kappa_m}$ are namely,the viscosity ratio, the Darcy number, the porous parameter, the modified internal Rayleigh number, the internal Rayleigh number and the diffusivity ratio for porous layer respectively. $W(z)$ & $W_m(z_m)$ are the vertical velocities, $\theta(z)$ & $\theta_m(z_m)$ are the temperature distributions and $S(z)$ & $S_m(z_m)$ are the concentration distributions in fluid and porous layers respectively and a and a_m are the horizontal wave numbers. Since the horizontal wave numbers must be the same for the composite layers, so that we have $\frac{a}{d} = \frac{a_m}{d_m}$ and hence $a_m = \widehat{d}a$, here $\widehat{d} = \frac{d_m}{d}$ is the depth ratio.

3. Boundary Conditions

The following boundary conditions are used to solve the equations (17)to (22) and they are

$$D^2W(1) + M_t a^2\theta(1) + M_s a^2 S(1) = 0 \tag{23}$$

The velocity boundary conditions are

$$\begin{aligned} &W(1) = 0, W_m(-1) = 0, D_m W_m(-1) = 0, \hat{T}W(0) = W_m(0),\\ &\hat{T}\hat{d}^2(D^2 + a^2)W(0) = \hat{\mu}(D_m^2 + a_m^2)W_m(0), \hat{T}\hat{d}DW(0) = D_m W_m(0)\\ &\hat{T}\hat{d}^3\beta^2[(D^3 - 3a^2D)]W(0) = [-D_m + \hat{\mu}\beta^2(D_m^3 - 3a_m^2 D_m)]W_m(0) \end{aligned} \tag{24}$$

Here, $\hat{T} = \frac{T_l - T_0}{T_0 - T_u}$, $M_t = -\frac{\partial\sigma_t}{\partial T}\frac{(T_0 - T_u)d}{\mu\kappa}$, $M_s = -\frac{\partial\sigma_t}{\partial C}\frac{(C_0 - C_u)d}{\mu\kappa}$ and σ_t are respectively the solute diffusivity ratio, the thermal ratio, the thermal Marangoni number, the solute Marangoni number and the surface tension.

4. Solution by Exact technique

The solutions of $W(z)$ and $W_m(z_m)$ are obtained by solving (17) and (20) using the velocity boundary conditions (24), as follows

$$W(z) = A_1[\cosh az + a_1 \sinh az + a_2 z\cosh az + a_3 z\sinh az] \tag{25}$$

$$W_m(z_m) = A_1[a_4\cosh a_m z_m + a_5 \sinh a_m z_m + a_6 \cosh\delta_m z_m + a_7\sinh\delta_m z_m] \tag{26}$$

where $\delta_m = \sqrt{a_m^2 + \frac{1}{\hat{\mu}\beta^2}}, a_1 = a_5\delta_1 + a_7\delta_2, a_2 = a_5\delta_1 + a_7\delta_6, a_3 = a_6\delta_3 + \delta_4,$

$a_4 = \hat{T} - a_6, a_5 = \frac{a_7\delta_7}{\delta_8}, a_6 = \frac{\delta_{11}\delta_{13} - \delta_{14}\delta_{10}}{\delta_9\delta_{13} - \delta_{12}\delta_{10}}, a_7 = \frac{\delta_{11}\delta_{12} - \delta_{14}\delta_9}{\delta_{10}\delta_{12} - \delta_9\delta_{13}},$

$\delta_1 = \frac{(1 + 3\hat{\mu}\beta^2 a_m^2)a_m}{2a^3\hat{T}\hat{d}^3\beta^2}, \delta_2 = \frac{(1 + 3\hat{\mu}\beta^2 a_m^2)\delta_m}{2a^3\hat{T}\hat{d}^3\beta^2}, \delta_3 = \frac{\hat{\mu}(\delta_m^2 - a_m^2)}{2a\hat{T}\hat{d}^2},$

$\delta_4 = \frac{\hat{\mu}a_m^2 - a^2\hat{d}^2}{a\hat{d}^2}, \delta_5 = \frac{a_m - a\hat{d}\hat{T}\delta_1}{\hat{T}\hat{d}}, \delta_6 = \frac{\delta_m - a\hat{d}\hat{T}\delta_2}{\hat{T}\hat{d}},$

$\delta_7 = a\hat{T}\hat{d}\delta_2 + \hat{T}\hat{d}\delta_6 - \delta_m, \delta_8 = a_m - a\hat{T}\hat{d}\delta_1 - \hat{T}\hat{d}\delta_5,$

$\delta_9 = \cosh\delta_m - \cosh a_m, \delta_{10} = -\sinh\delta_m - \frac{\delta_7 \sinh a_m}{\delta_8},$

$\delta_{11} = -\hat{T}\cosh a_m, \delta_{12} = a_m \sinh a_m - \delta_m \sinh \delta_m,$
$\delta_{13} = \dfrac{\delta_7 a_m \cosh a_m}{\delta_8} + \delta_m \cosh \delta_m, \delta_{14} = \hat{T} a_m \sinh a_m$
Solving equations (19) and (22) for the salinity distributions $S(z)$ and $S_m(z_m)$ using the following salinity/concentration boundary conditions, which are as follows

$$DS(1) = 0, S(0) = \hat{S}S_m(0), DS(0) = D_m S_m(0), D_m S_m(-1) = 0 \tag{27}$$

where $\hat{S} = \dfrac{C_l - C_0}{C_0 - C_u}$ is the solutal ratio, the concentration distributions $S(z)$ and $S_m(z_m)$ are obtained using the concentration boundary conditions (27), as follows

$$S(z) = A_1[c_{13}\cosh az + c_{14}\sinh az + f_1(z)] \tag{28}$$
$$S_m(z_m) = A_1[c_{15}\cosh a_m z_m + c_{16}\sinh a_m z_m + f_{m1}(z_m)] \tag{29}$$

where $f_1(z) = \dfrac{-1}{\tau}[\dfrac{z}{2a}(a_1 \cosh az + \sinh az) + R_9],$
$R_9 = \dfrac{z^2}{4a}(a_3 \cosh az + a_2 \sinh az) - \dfrac{z}{4a^2}(a_2 \cosh az + a_3 \sinh az),$
$f_{m1}(z_m) = \dfrac{-1}{\tau_{pm}}[\dfrac{z_m}{2a_m}(a_5 \cosh a_m z_m + a_4 \sinh a_m z_m) + R_{10}],$
$R_{10} = \dfrac{z_m}{2\delta_m}(a_7 \cosh \delta_m z_m + a_6 \sinh \delta_m z_m),$
$c_{13} = \widehat{S}c_{15}, c_{14} = \dfrac{1}{a}(c_{16}a_m + \Delta_{101} - \Delta_{102}),$
$c_{15} = \dfrac{\Delta_{106} a_m \cosh a_m - \Delta_{103}\Delta_{105}}{\Delta_{105} a_m \sinh a_m + \Delta_{104} a_m \cosh a_m},$
$c_{16} = \dfrac{\Delta_{103}\Delta_{104} + \Delta_{106} a_m \sinh a_m}{\Delta_{104} a_m \cosh a_m + \Delta_{105} a_m \sinh a_m},$
$\Delta_{100} = -\dfrac{1}{\tau}[\dfrac{1}{2}(\cosh a + a_1 \sinh a) + \dfrac{1}{2a}(a_1 \cosh a + \sinh a) + R_{27}],$
$R_{27} = \dfrac{(a^2-1)}{4a^2}(a_2 \cosh a + a_3 \sinh a) + \dfrac{1}{4a}(a_3 \cosh a + a_2 \sinh a),$
$\Delta_{101} = -\dfrac{1}{\tau_{pm}}[\dfrac{a_5}{2a_m} + \dfrac{a_7}{2\delta_m}], \Delta_{102} = -\dfrac{1}{\tau}[\dfrac{a_1}{2a} - \dfrac{a_2}{4a^2}],$
$\Delta_{103} = \dfrac{1}{\tau_{pm}}[\dfrac{-1}{2}(a_4 \cosh a_m - a_5 \sinh a_m) + R_{28} - R_{29} + R_{30}]$
$R_{28} = \dfrac{1}{2a_m}(a_5 \cosh a_m - a_4 \sinh a_m)$
$R_{29} = \dfrac{1}{2}(a_6 \cosh \delta_m - a_7 \sinh \delta_m)$
$R_{30} = \dfrac{1}{2\delta_m}(a_7 \cosh \delta_m - a_6 \sinh \delta_m), \Delta_{104} = a\widehat{S}\sinh a,$
$\Delta_{105} = a_m \cosh a, \Delta_{106} = \Delta_{100} - (\Delta_{101} - \Delta_{102})\cosh a$

5. Thermal Marangoni number

5.1. Type (I): Adiabatic-Adiabatic. Solving equations (18) and (21) for the temperature distributions $\theta(z)$ and $\theta_m(z_m)$ using the following temperature boundary conditions, where both the boundaries are adiabatic and the heat and heat flux are continuous at the interface, which are as follows

$$D\theta(1) = 0, \theta(0) = \hat{T}\theta_m(0), D\theta(0) = D_m\theta_m(0), D_m\theta_m(-1) = 0 \tag{30}$$

The temperature distributions $\theta(z)$ and $\theta_m(z_m)$ are obtained using the temperature boundary conditions (30), as follows

$$\theta(z) = A_1[c_1 \cosh az + c_2 \sinh az + g_1(z)] \tag{31}$$

$$\theta_m(z_m) = A_1[c_3 \cosh a_m z_m + c_4 \sinh a_m z_m + g_{m1}(z_m)] \tag{32}$$

where

$g_1(z) = A_1[\Delta_1 - \Delta_2 + \Delta_3 - \Delta_4], g_{m1}(z_m) = A_1[\Delta_5 - \Delta_6 + \Delta_7 - \Delta_8]$

$\Delta_1 = \dfrac{(2E_1 z + E_2 z^2)}{4a}(a_1 \cosh az + \sinh az)$

$\Delta_2 = \dfrac{E_2 z}{4a^2}(\cosh az + a_1 \sinh az)$

$\Delta_3 = \dfrac{(6a^2 z^2 E_1 + 4a^2 z^3 E_2 + 6E_2 z)}{24a^3}(a_3 \cosh az + a_2 \sinh az)$

$\Delta_4 = \dfrac{(E_1 z + E_2 z^2)}{4a^2}(a_2 \cosh az + a_3 \sinh az)$

$\Delta_5 = \dfrac{(2E_{1m} z_m + E_{2m} z_m^2)}{4a_m}(a_5 \cosh a_m z_m + a_4 \sinh a_m z_m)$

$\Delta_6 = \dfrac{E_{2m} z_m}{4a_m^2}(a_4 \cosh a_m z_m + a_5 \sinh a_m z_m)$

$\Delta_7 = \dfrac{(2E_{1m} z_m + E_{2m} z_m^2)}{4\delta_m}(a_7 \cosh \delta_m z_m + a_6 \sinh \delta_m z_m)$

$\Delta_8 = \dfrac{E_{2m} z_m}{4\delta_m^2}(a_6 \cosh \delta_m z_m + a_7 \sinh \delta_m z_m)$

$E_1 = R_I^* - 1, E_2 = -2R_I^*, E_{1m} = -(R_{Im}^* + 1), E_{2m} = -2R_{Im}^*$

$c_1 = c_3\widehat{T}, c_2 = \dfrac{1}{a}(c_4 a_m + \Delta_{10} - \Delta_{11}),$

$c_3 = \dfrac{\Delta_{14}\Delta_{16} - \Delta_{17}\Delta_{12}}{\Delta_{13}\Delta_{16} - \Delta_{15}\Delta_{12}}, c_4 = \dfrac{\Delta_{14}\Delta_{15} - \Delta_{17}\Delta_{13}}{\Delta_{12}\Delta_{15} - \Delta_{16}\Delta_{13}},$

$\Delta_9 = -A_1[R_1 + R_2 + R_3 + R_4]$

$R_1 = \dfrac{(2a^2 E_1 + E_2(a^2 - 1))}{4a^2}(\cosh a + a_1 \sinh a)$

$R_2 = \dfrac{E_2 + 2E_1}{4a}(a_1 \cosh a + \sinh a)$

$R_3 = \dfrac{(3a^2 - 3)E_1 + (2a^2 - 3)E_2}{12a^2}(a_2 \cosh a + a_3 \sinh a)$

$R_4 = \dfrac{(a^2 E_1 + E_2(a^2 + 1))}{4a^3}(a_3 \cosh a + a_2 \sinh a)$

$\Delta_{10} = \frac{2E_{1m}a_5}{4a_m} - \frac{a_4 E_{2m}}{4a_m^2} + \frac{2E_{1m}a_7}{4\delta_m} - \frac{a_6 E_{2m}}{4\delta_m^2}$
$\Delta_{11} = \frac{(2a^2 a_1 - aa_2)E_1 + (a_3 - a)E_2}{4a^3}, \Delta_{12} = a_m \cosh a_m,$
$\Delta_{13} = -a_m \sinh a_m, \Delta_{14} = -[R_5 + R_6 + R_7 + R_8],$
$R_5 = [\frac{E_{2m} - 2E_{1m}}{4} - \frac{E_{2m}}{4a_m^2}](a_4 \cosh a_m - a_5 \sinh a_m),$
$R_6 = \frac{2E_{1m} - E_{2m}}{4a_m}](a_5 \cosh a_m - a_4 \sinh a_m)$
$R_7 = [\frac{E_{2m} - 2E_{1m}}{4} - \frac{E_{2m}}{4\delta_m^2}](a_6 \cosh \delta_m - a_7 \sinh \delta_m),$
$R_8 = [\frac{2E_{1m} - E_{2m}}{4\delta_m}](a_7 \cosh \delta_m - a_6 \sinh \delta_m),$
$\Delta_{15} = a\widehat{T} \sinh a, \Delta_{16} = a_m \cosh a, \Delta_{17} = \Delta_9 - (\Delta_{10} - \Delta_{11}) \cosh a$
From the boundary condition (23), we have

$$M_t = -[\frac{D^2W(1) + M_s a^2 S(1)}{a^2\theta(1)}]$$

The thermal Marangoni number as follows

$$M_{t1} = -\frac{[\Lambda_1 + \Lambda_2 + \Lambda_3]}{a^2(c_1 \cosh a + c_2 \sinh a + \Lambda_4 + \Lambda_5)} \tag{33}$$

where
$\Lambda_1 = a^2(\cosh a + a_1 \sinh a) + a_2(a^2 \cosh a + 2a \sinh a) + a_3(a^2 \sinh a + 2a \cosh a)$
$\Lambda_2 = -\frac{1}{\tau}[\frac{1}{2a}(a_1 \cosh a + \sinh a) + \frac{1}{4a}(a_3 \cosh a + a_2 \sinh a)],$
$\Lambda_3 = \frac{1}{\tau}[\frac{1}{4a^2}(a_2 \cosh a + a_3 \sinh a)],$
$\Lambda_4 = \frac{(E_2 + E_1)}{4a}(a_1 \cosh a + \sinh a) - \frac{E_2}{4a^2}(\cosh a + a_1 \sinh a)$
$\Lambda_5 = \frac{(4a^2E_2 + 6a^2E_1 + 6E_2)}{24a^3}(a_3 \cosh a + a_2 \sinh a)$
$- \frac{(E_2 + E_1)}{4a^2}(a_2 \cosh a + a_3 \sinh a)$

5.2. Type (II): Adiabatic-Isothermal. Solving equations (18) and (21) for the temperature distributions $\theta(z)$ and $\theta_m(z_m)$ using the following temperature boundary conditions, where the upper boundary of the fluid layer is adiabatic and the lower boundary of the porous layer is isothermal and at the interface, heat and heat flux are continuous which are as follows

$$D\theta(1) = 0, \theta(0) = \hat{T}\theta_m(0), D\theta(0) = D_m\theta_m(0), \theta_m(-1) = 0 \tag{34}$$

The temperature distributions $\theta(z)$ and $\theta_m(z_m)$ are obtained using the temperature boundary conditions (34), as follows

$$\theta(z) = A_1[c_5 \cosh az + c_6 \sinh az + g_2(z)] \tag{35}$$

$$\theta_m(z_m) = A_1[c_7 \cosh a_m z_m + c_8 \sinh a_m z_m + g_{m2}(z_m)] \tag{36}$$

where

$g_2(z) = A_1[R_{11} - R_{12} + R_{13} - R_{14}], g_{m2}(z_m) = A_1[R_{15} - R_{16} + R_{17} - R_{18}]$

$R_{11} = \dfrac{(2E_3 z + E_4 z^2)}{4a}(a_1 \cosh az + \sinh az)$

$R_{12} = \dfrac{E_4 z}{4a^2}(\cosh az + a_1 \sinh az)$

$R_{13} = \dfrac{(6a^2 z^2 E_3 + 4a^2 z^3 E_4 + 6E_4 z)}{24a^3}(a_3 \cosh az + a_2 \sinh az)$

$R_{14} = \dfrac{(E_3 z + E_4 z^2)}{4a^2}(a_2 \cosh az + a_3 \sinh az)$

$R_{15} = \dfrac{(2E_{3m} z_m + E_{4m} z_m^2)}{4a_m}(a_5 \cosh a_m z_m + a_4 \sinh a_m z_m)$

$R_{16} = \dfrac{E_{4m} z_m}{4a_m^2}(a_4 \cosh a_m z_m + a_5 \sinh a_m z_m)$

$R_{17} = \dfrac{(2E_{3m} z_m + E_{2m} z_m^2)}{4\delta_m}(a_7 \cosh \delta_m z_m + a_6 \sinh \delta_m z_m)$

$R_{18} = \dfrac{E_{4m} z_m}{4\delta_m^2}(a_6 \cosh \delta_m z_m + a_7 \sinh \delta_m z_m)$

$E_3 = R_I^* - 1, E_4 = -2R_I^*, E_{3m} = -(R_{Im}^* + 1), E_{4m} = -2R_{Im}^*$

$c_5 = c_7 \widehat{T}, c_6 = \dfrac{1}{a}(c_8 a_m + \Delta_{19} - \Delta_{20}),$

$c_7 = \dfrac{\Delta_{23}\Delta_{25} + \Delta_{26}\Delta_{22}}{\Delta_{21}\Delta_{25} + \Delta_{24}\Delta_{22}}, c_8 = \dfrac{\Delta_{26}\Delta_{21} - \Delta_{23}\Delta_{24}}{\Delta_{22}\Delta_{24} + \Delta_{25}\Delta_{21}},$

$\Delta_{18} = -A_1[R_{19} + R_{20} + R_{21} + R_{22}]$

$R_{19} = \dfrac{(2a^2 E_3 + E_4(a^2 - 1))}{4a^2}(\cosh a + a_1 \sinh a)$

$R_{20} = \dfrac{E_4 + 2E_3}{4a}(a_1 \cosh a + \sinh a)$

$R_{21} = \dfrac{(3a^2 - 3)E_3 + (2a^2 - 3)E_4}{12a^2}(a_2 \cosh a + a_3 \sinh a)$

$R_{22} = \dfrac{(a^2 E_3 + E_4(a^2 + 1))}{4a^3}(a_3 \cosh a + a_2 \sinh a)$

$\Delta_{19} = \dfrac{2E_{3m} a_5}{4a_m} - \dfrac{a_4 E_{4m}}{4a_m^2} + \dfrac{2E_{3m} a_7}{4\delta_m} - \dfrac{a_6 E_{4m}}{4\delta_m^2}$

$\Delta_{20} = \dfrac{(2a^2 a_1 - a a_2)E_3 + (a_3 - a)E_4}{4a^3}, \Delta_{21} = \cosh a_m,$

$\Delta_{22} = \sinh a_m, \Delta_{23} = -[R_{23} + R_{24} + R_{25} + R_{26}],$

$R_{23} = [\dfrac{E_{4m} - 2E_{3m}}{4a_m}](a_5 \cosh a_m - a_4 \sinh a_m),$

$R_{24} = \dfrac{E_{4m}}{4a_m^2}(a_4 \cosh a_m - a_5 \sinh a_m)$

$R_{25} = [\dfrac{E_{4m} - 2E_{3m}}{4\delta_m}](a_7 \cosh \delta_m - a_6 \sinh \delta_m),$

$R_{26} = [\dfrac{E_{4m}}{4\delta_m^2}](a_6 \cosh \delta_m - a_7 \sinh \delta_m),$

$\Delta_{24} = a\widehat{T}\sinh a, \Delta_{25} = a_m \cosh a, \Delta_{26} = \Delta_{18} - (\Delta_{19} - \Delta_{20})\cosh a$
From the boundary condition (23), we have

$$M_t = -[\frac{D^2W(1) + M_s a^2 S(1)}{a^2\theta(1)}]$$

The thermal Marangoni number as follows

$$M_{t2} = -\frac{[\Lambda_1 + \Lambda_2 + \Lambda_3]}{a^2(c_1\cosh a + c_2\sinh a + \Lambda_6 + \Lambda_7)} \tag{37}$$

where

$\Lambda_1 = a^2(\cosh a + a_1\sinh a) + a_2(a^2\cosh a + 2a\sinh a) + a_3(a^2\sinh a + 2a\cosh a)$

$\Lambda_2 = -\frac{1}{\tau}[\frac{1}{2a}(a_1\cosh a + \sinh a) + \frac{1}{4a}(a_3\cosh a + a_2\sinh a)],$

$\Lambda_3 = \frac{1}{\tau}[\frac{1}{4a^2}(a_2\cosh a + a_3\sinh a)],$

$\Lambda_6 = \frac{(E_4 + E_3)}{4a}(a_1\cosh a + \sinh a) - \frac{E_4}{4a^2}(\cosh a + a_1\sinh a)$

$\Lambda_7 = \frac{(4a^2E_4 + 6a^2E_3 + 6E_4)}{24a^3}(a_3\cosh a + a_2\sinh a)$
$- \frac{(E_4 + E_3)}{4a^2}(a_2\cosh a + a_3\sinh a)$

6. Results and Discussion

The thermal Marangoni numbers M_{t1} and M_{t2} for the Types (I) and (II) Temperature Boundary Combinations (TBC) are obtained theoretically in terms of $\hat{d}, \beta, M_s, R_I^*, R_{Im}^*, \hat{\mu}$ and τ which are respectively, the depth ratio, the porous parameter, the solute Marangoni number, the modified internal Rayleigh numbers in fluid and porous regions, the viscosity ratio and the solute diffusivity ratio. The thermal Marangoni numbers are drawn as a function of depth ratio for the set of parameters $a = 0.5, \beta = 5.0, \tau = \tau_{pm} = 0.10, \hat{T} = 0.1, \hat{S} = 0.1, \hat{\mu} = 2.5, M_s = 50, R_I^* = 1$and $R_{Im}^* = 1$.
Figure 2, represents the comparison of M_{t1} and M_{t2}, where $\log(M_{t1} \& M_{t2})$ is the dependent variable and $\hat{d}$, the depth ratio is independent variable. The thermal Marangoni number decreases up to some value of depth ratio, later it increases as the value of depth ratio increases. This behavior is qualitatively same for both Types of TBC. It is interesting to note that for larger values of depth ratios, the Marangoni numbers coincide and no change in them for $\hat{d} \geq 5$, i.e., for porous layer dominant (in depth) systems which is physically impressive as the TBC at the boundary of the porous layer is changed. But for the smaller depth ratio values, the thermal Marangoni number for Type (I) is larger than that for Type (II), indicating that the system with Type (I) TBC is more stable. The essence of these parameters on the thermal Marangoni numbers, hence on Benard double diffusive Marangoni convection for Types (I) and (II) are presented graphically by varying the corresponding parameter for fixed values of other parameters using Darcy-Brinkmann model in figures (a) and (b) respectively.

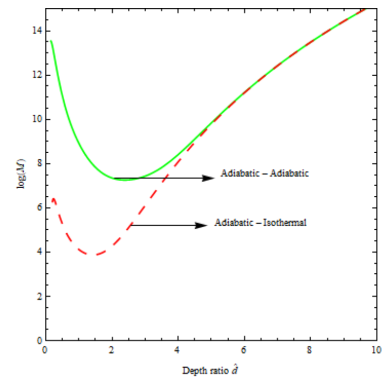

FIGURE 2. Comparison of thermal Marangoni numbers for Type (I) (Adiabatic-Adiabatic) and Type (II) (Adiabatic-Isothermal)

Figure 3 demonstrates the effects of porous parameter on the thermal Marangoni number, hence on the Benard double diffusive Marangoni convection. The values of supplementary parameters are fixed and they are $a = 0.5, \tau = \tau_{pm} = 0.10, \hat{T} = 0.1, \hat{S} = 0.1, \hat{\mu} = 2.5, M_s = 50, R_I^* = 1$ and $R_{Im}^* = 1$ and the values of $\beta = 5.0, 10.0, 15.0$. For a fixed depth ratio, the change in the porous parameter is actually change in permeability of the porous region. Increasing porous parameter means there is more window for the fluid to move. It quite interesting to note that the behavior of the eigenvalue is qualitatively similar for smaller depth ratios. The converging curves for Type (I) TBC indicate that no effect of porous parameter on the system with Type (I) TBC for larger values of depth ratios. For fluid layer dominant systems, for a fixed value of depth ratio, the increase in the value of porous parameter, increases the thermal Marangoni number, which is not expected, and this may be due to the presence of second diffusing component.

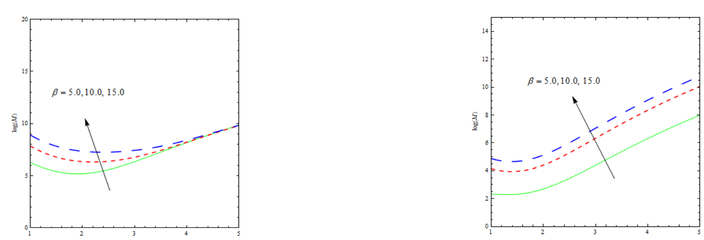

(a) (b)

FIGURE 3. The effects of porous parameter β

Figure 4, which explains the influence of solute Marangoni number on the Benard double diffusive Marangoni convection for $M_s = 5.0, 10.0, 50.0$. The increase in the solute Marangoni number is to increase the thermal Marangoni number hence its effects is to delay the onset of non-Darcian-Benard double diffusive Marangoni convection in a composite layer. The effect of this parameter is same on the systems with both the types of TBCs.

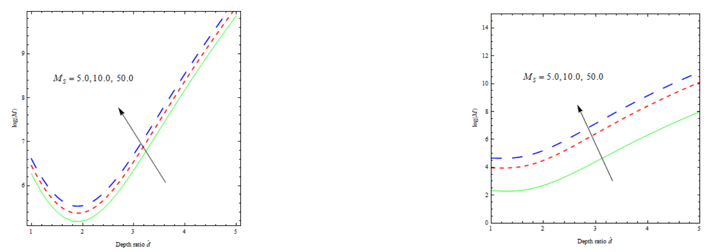

(a) (b)

FIGURE 4. The effects of solute Marangoni number M_s

The effects of viscosity ratio $\hat{\mu}$ on the Eigen value is shown in Figure 5 for $\hat{\mu} = 1.0, 1.5, 2.0$ and other parameters are $a = 0.5, \beta = 5.0, \tau = \tau_{pm} = 0.10, \hat{T} = 0.1, \hat{S} = 0.1, M_s = 50, R_I^* = 1$ and $R_{Im}^* = 1$. For both the types of TBCs, the curves are diverging which indicates that the impact of $\hat{\mu}$ is more for larger depth ratios, that is for systems with broader porous regions. For a fixed depth ratio, increase in the ratio of the effective viscosity of the fluid in the porous region to that in the fluid region, increases the thermal Marangoni number hence, the non-Darcian-Benard double diffusive Marangoni convection is delayed.

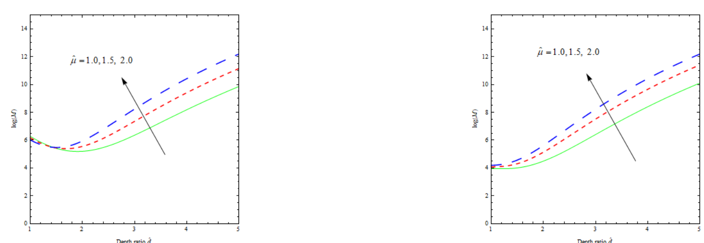

(a) (b)

FIGURE 5. The effects of viscosity ratio $\widehat{\mu}$

The essence of heat source/sink in the fluid region is explained by the modified internal Rayleigh number and the effect of the same is shown in Figure 6 for $R_I^* = -1.0, 0.0, 1.0$ and other parameters are $a = 0.5, \beta = 5.0, \tau = \tau_{pm} =$

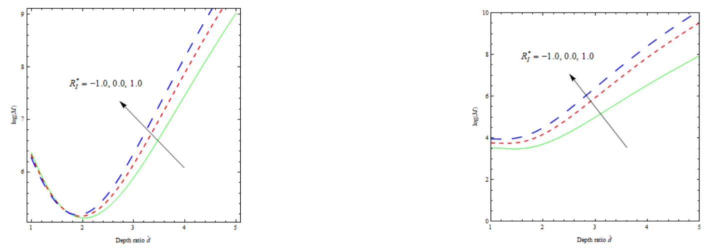

(a) (b)

FIGURE 6. Effects of modified internal Rayleigh number R_I^*

$0.10, \hat{T} = 0.1, \hat{S} = 0.1, \hat{\mu} = 2.5, M_s = 50$ and $R_{Im}^* = 1$. The negative value of R_I^* denotes the sink and the positive value of R_I^* means the source. The diverging curves for both the types of TBCs reveal that the impact of R_I^* is more effective for porous layer dominant systems. For a fixed depth ratio, the increase in the value of internal Rayleigh number (sink to source), increases the thermal Marangoni number which is physically meaningful. So larger number of R_I^* are suitable for the situations controlling non-Darcian-Benard double diffusive Marangoni convection.

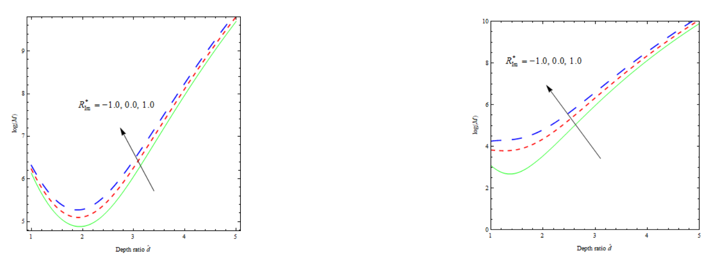

(a) (b)

FIGURE 7. Effects of modified internal Rayleigh number R_{Im}^*

Figure 7 demonstrates the effect of modified internal Rayleigh number R_{Im}^* on the stability of the system for $R_{Im}^* = -1.0, 0.0, 1.0$ and other parameters are $a = 0.5, \beta = 5.0, \tau = \tau_{pm} = 0.10, \hat{T} = 0.1, \hat{S} = 0.1, \hat{\mu} = 2.5, M_s = 50$ and $R_I^* = 1$. The diverging curves for both the types of TBCs reveal that the impact of R_{Im}^* is more effective for porous layer dominant systems. For a fixed depth ratio, the increase in the value of internal Rayleigh number, that is from sink to source, increases the thermal Marangoni number. So larger number of R_{Im}^* are suitable for the situations controlling non-Darcian-Benard double diffusive Marangoni convection.

The effects of the diffusivity ratio τ on the non-Darcian-Benard double diffusive

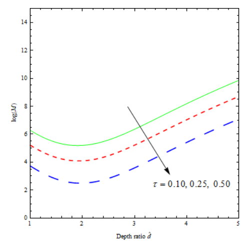

(a)

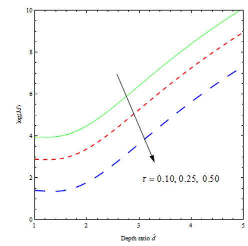

(b)

FIGURE 8. Effects of diffusivity ratio τ

Marangoni convection is displayed in Figure 8, for $\tau = 0.10, 0.25, 0.50$ and other parameters are $a = 0.5, \beta = 5.0, \tau_{pm} = 0.10, \hat{T} = 0.1, \hat{S} = 0.1, \hat{\mu} = 2.5, M_s = 50, R_I^* = 1$ and $R_{Im}^* = 1$.The effect of this parameter is uniform for all depth ratios for both types of TBCs. For a fixed depth ratio, the increase in the value of diffusivity ratio decreases the thermal Marangoni number hence it is an important parameter which can accelerate the non-Darcian-Benard double diffusive Marangoni convection.

7. Conclusions

The findings from this study are

(1) The TBC Type (I) can be utilized in the situations where non Darcian Benard double diffusive Marangoni convection in a two layer system, needs to be controlled, whereas Type (II) TBC is conducive for situations where the same is to be accelerated.
(2) Higher values of porous parameter, solute Marangoni number, viscosity ratio, internal Rayleigh number and lower values of diffusivity ratio can delay non-Darcian-Benard double diffusive Marangoni convection.
(3) Heat source/sink plays an important role on convection, by choosing an appropriate the strength of the heat source, onset of non-Darcian-Benard double diffusive Marangoni convection can be augmented or delayed.

Conflict of Interest : Authors have no conflicts of interest

References

1. Akil J. Harfash., Fahad K. Nashmi., *Triply resonant double diffusive convection in a fluid layer*, Mathematical Modelling and Analysis **22** (2017), 809-826.
2. A.C. Baytas, A.F. Baytas, D.B. Ingham, I. Pop, *Double diffusive natural convection in an enclosure filled with a step type porous layer: Non-Darcy flow*, International Journal of Thermal Sciences **48** (2009), 665-673.
3. S. Habibis, H. Ishak, *Non-Darcy and localized heating effects on Benard convection in porous enclosure*, Journal of Porous Media **16** (2013), 1-10.

4. Khaled Al-Farhany and A. Turan, *Numerical study of double diffusive natural convective heat and mass transfer in an inclined rectangular cavity filled with porous medium*, International Communications in Heat and Mass Transfer **39** (2012), 174-181.
5. Khaled Al-Farhany and Ali Turan, *Double-Diffusive of natural convection in an inclined porous square domain generalized model*, Al-Qadisiyah Journal for Engineering Sciences **12** (2019), 151-160.
6. A. Khalili, I.S. Shivakumara, *Non-Darcian effects on the onset of convection in a porous layer with Throughflow*, Transport in Porous Media **53** (2003), 245-263.
7. Khanafer K., Vafai K., *Double-diffusive mixed convection in a lid-driven enclosure filled with a fluid-saturated porous medium*, Numerical Heat Transfer, Part A: Applications **42** (2002), 465-486.
8. Krishna B. Chavaraddi, *Marangoni convection in a composite porous layer and a fluid layer with a deformable free surface*, International Journal of Fluid Mechanics Research **34** (2007), 352-373.
9. N. Manjunatha, R. Sumithra, *Effects of non-uniform temperature gradients on double diffusive Marangoni convection in a two layer system*, International Journal of Pure and Applied Mathematics **118** (2018), 203-220.
10. N. Manjunatha, R. Sumithra, *Effects of heat source/sink and non uniform temperature gradients on Benard-surface tension driven convection in a composite layer in the presence of vertical magnetic field*, Gedrag en Organisatie **33** (2020), 865-879.
11. Muneer A. Ismael, Ali J. Chamkha, *Conjugate natural convection in a differentially heated composite enclosure filled with a nanofluid*, Journal of Porous Media **18** (2015), 699-716.
12. D.A. Nield, A. Bejan, *Convection in Porous Media*, Fourth Edition, In: Convection in Porous Media Springer, 2013.
13. Rashmi Dubey, P.V.S.N. Murthy, *The onset of double-diffusive convection in a Brinkman porous layer with convective thermal boundary conditions*, AIP Advances **9** (2019), 045322.
14. S. Safi, S. Benissaad, *Double-diffusive convection in an anisotropic porous layer using the Darcy-Brinkman-Forchheimer formulation*, Arch. Mech. **70** (2018), 89-102.
15. M. Sankar, Youngyong Park, J.M. Lopez, Younghae Do, *Numerical study of natural convection in a vertical porous annulus with discrete heating*, International Journal of Heat and Mass Transfer **54** (2011), 1493-1505.
16. M. Sankar, Junpyo Park, Dongseok Kim, Younghae Do, *Numerical study of natural convection in a vertical porous annulus with an internal heat source: Effect of Discrete Heating*, Numerical Heat Transfer, Part A: Applications **63** (2013), 687-712.
17. I.S. Shivakumara, R. Sumithra, *Non-Darcian effects on double diffusive convection in a sparsely packed porous medium*, Acta Mechanica **132** (1999), 113-127.

N. Manjunatha received M.Sc. from Bangalore University, M.Phil. from Alagappa University and Ph.D. from Bharathiar University. He is currently working as Assistant Professor at REVA University, Bengaluru since 2009. His research interests include Fluid Mechanics, Heat & Mass transfer, MHD and Convection stability analysis.

Department of Mathematics, School of Applied Sciences, REVA University, Bengaluru-560064, India.
e-mail: manjunatha.n@reva.edu.in

R. Sumithra received M.Sc., M.Phil. and Ph.D. from Bangalore University. She is currently working as Associate Professor at Government Science College Autonomous, Bengaluru since 2002. Her research interests are Fluid Mechanics and MHD.

Department of UG, PG Studies & Research in Mathematics, Government Science College Autonomous, Bengaluru-560001, India.
e-mail: sumitra_diya@yahoo.com

R.K. Vanishree received M.Sc. and Ph.D. from Bangalore University. She is currently Associate professor at Maharani's Science College for Women, Maharani's Cluster University. Her research interests are Fluid Mechanics and MHD.

Department of Mathematics, Maharani's Science College for Women, Maharani's Cluster University, Bengaluru-560001, India.
e-mail: vanirkmscw@gmail.com